Gargallo Bellés, S.; Martín Monerris, M.; Oliver Rajadel, N.; Hernández Crespo, C. (2017). Biokinetic model for nitrogen removal in free water surface constructed wetlands. The Science of The Total Environment. 587:145-156. doi:10.1016/j.scitotenv.2017.02.089

Biokinetic model for nitrogen removal in free water surface constructed wetlands

S. Gargallo[1]*, M. Martín[1], N. Oliver[1], C. Hernández-Crespo[1]

[1]Research Institute of Water and Environmental Engineering

Universitat Politècnica de València, Cno. de Vera s/n, Valencia, Spain

sagarbel@upv.es

Keywords: mathematical modelling; ASM; eutrophic water; nitrification; denitrification; plant uptake.

Abstract

In this article, a mechanistic biokinetic model for nitrogen removal in free water surface constructed wetlands treating eutrophic water was developed, including organic matter performance due to its importance in nitrogen removal by denitrification. Ten components and fourteen processes were introduced in order to simulate the forms of nitrogen and organic matter, the mechanisms of autotrophic and heterotrophic microorganisms in both aerobic and anoxic conditions, as well as macrophytes nitrogen uptake and release. Dissolved oxygen was introduced as an input variable with a time step of 0.5 days for mimicking eutrophic environments: aerobic conditions were assigned during daylight hours and anoxic conditions during the night. The sensitivity analysis showed that the most influential parameters were those related to the growth of heterotrophic and autotrophic microorganisms. The model was properly calibrated and validated in two full scale systems working in real conditions for treating eutrophic water from Lake L´Albufera (València). In the studied systems, ammonium was mainly removed by the growth of autotrophic microorganisms (nitrification) whereas nitrate was removed by the anoxic growth of heterotrophic microorganisms (denitrification). Macrophyte uptake removed between 9-19% of the ammonium entering to the systems, although degradation of dead standing macrophytes returned a significant part to water column.

1. Introduction

During last decades, multiple efforts have been done in order to preserve natural water bodies from eutrophication. Reducing nutrient loads (mainly, nitrogen and phosphorus) by treating urban wastewater was an important step, but in some cases it was demonstrated to be insufficient for recovering water quality in eutrophicated systems (Martín et al., 2013). For example, in Sweden, where one of the major problems for surface water is eutrophication caused by the diffuse pollution from agricultural sources, 1574 constructed wetlands (CWs) were built between 1996 and 2006 with the aim of reducing agricultural runoff and restoring the Baltic Sea good ecological status (Arheimer and Pers, 2016). Furthermore, some experiences carried out worldwide have demonstrated the usefulness of CWs, both free water surface (FWSCWs) and subsurface flow (SSFCWs) configurations, for treating eutrophic water in order to remove nutrients and phytoplankton biomass (He et al., 2007; Li et al., 2008; Martín et al., 2013; Tang et al., 2009).

CWs efficiency removal depends on a large amount of factors (e.g. inlet concentrations, loading rates, hydraulic configuration, vegetation cover, temperature and pH) whose influence can be different for each process. Given the complex task of taking into account the numerous interdependencies, modelling has been demonstrated to be a useful tool for simulating the performance of these systems and many typologies of models have been recently developed. Among them all, mechanistic or process-based models are considered to be the most useful for understanding systems performance (Langergraber, 2008). The vast majority of process-based models have been developed for simulating SSFCWs treating wastewater, being CWM1 (Langergraber et al., 2009), CW2D (Langergraber and Šimůnek, 2005) and BIO-PORE (Samsó and Garcia, 2013) some of the most robust and widely accepted. However, this kind of models are less abundant for simulating FWSCWs and some of the available ones, such as Galanopoulos and Lyberatos (2016), include a limited number of components and interactions. Specifically, seven components and five processes are used in this model for simulating eutrophic water treatment in FWSCWs including nitrogen and organic matter forms, whereas phosphorus influence and interactions between water column and sediment layer were not considered.

One of the most complete models for FWSCWs was developed by Gargallo et al. (2016), where total suspended solids, phytoplankton and phosphorus in eutrophic water were simulated taking into account the effects of avifauna and wind in resuspension processes, as well as vegetation cover (VC) in resuspension and sedimentation mechanisms. In this model, Gargallo et al. considered both organic and total inorganic phosphorus (OP and TIP,

respectively, mg P L^{-1}) and the last one was divided into soluble (DIP, dissolved inorganic phosphorus) and particulate (PIP, particulate inorganic phosphorus) fractions. Furthermore, phosphorus accumulated inside the phytoplankton cells was simulated by means of the component P_{int} (mg P mg Chl a^{-1}).

However, nitrogen forms and nutrient uptake by plants were not included in this model.

The aim of this paper is (1) to develop a process-based model for nitrogen performance in free water surface constructed wetlands treating eutrophic water, (2) to calibrate and validate it in two full-scale systems working in real conditions and (3) to look into the main processes in relation to nitrogen removal, focusing mainly in nitrate and ammonium.

2. Methods

2.1 Site description and experimental data

Experimental data for calibrating and validating the model was collected in a set of two FWSCWs located in the natural reserve area known as *Tancat de la Pipa*, in València (Spain). Calibration was carried out in the unit named as FG1 (13509 m^2) and validation in FG2 (18240 m^2). These FWSCWs, which were planted with cattails (*Thypa* spp.), operated in series in order to treat hypertrophic water from lake L´Albufera.

These systems were monitored from April 2009 to April 2012. During these three years they worked continuously, except in three periods that water input was stopped due to maintenance tasks. More details about CWs configuration and functioning can be found in Martín et al. (2013).

Three points were studied for water quality: P0 at the inlet to FG1 and P1 and P2 at the outlet of FG1 and FG2, respectively. They were monitored every two weeks from April 2009 to October 2011, and monthly from November 2011 to April 2012 (n=64). Water samples were collected in 2L bottles, transported and preserved at 4ºC until they were analysed in laboratory, no later than 24 h. Ammonium, nitrate, nitrite, total nitrogen (TN), soluble and total chemical oxygen demand (COD_S and COD_T, respectively) were measured using the Spectroquant® Analysis System by Merck, while dissolved oxygen (DO), pH and temperature were measured *in situ* using portable field measurement equipment (WTW-Multi 340i). Phosphates, total phosphorus, phytoplankton and total suspended solids, as well as inflow, outflow, meteorological data and VC estimations obtained in Gargallo et al. (2016) and Martín et al. (2013) were used as input data for calibrating and validating the model.

In order to establish the fractioning of the organic matter measurements into the organic components of the model (S_S, S_i, X_S and X_i, see Table 1 in next section) one test was carried out in point P0 in February 2010. Particulate and soluble COD and BOD_5 were measured in P0 (COD_P=18.2, COD_S=19.8, particulate BOD_5=16.0, soluble BOD_5=3.9 mg O_2 L^{-1}, respectively). Assuming that soluble BOD_5 corresponds to S_s and total BOD_5 to the sum of S_s and X_s, it was obtained that X_s and X_i correspond to 88% and 12% of COD_P, respectively, whereas S_s and S_i to 20% and 80% of COD_S. These percentages were applied to COD_T and COD_S measured in the FWSCWs during the studied period.

Once per season, from December 2011 to September 2012, DO and pH were measured every 15 minutes for 24 hours in points P0, P1 and P2. In these point, alkalinity was measured every three weeks from July to December 2015 (n=8) using the methodology by APHA (1991).

2.2 Model development

The Activated Sludge Model series structure (Henze et al., 2000) was used for representing the processes involved in nitrogen removal. Matrix notation was used to represent the effect of each process on each component by means of the specific stoichiometric coefficients and processes kinetic rates. Components included in the model are listed in Table 1. The capital letter S was used for denoting soluble components and X for particulate ones. Following CWM1 (Langergraber et al., 2009), S_{NO3} was assumed to include the sum of nitrite and nitrate concentrations and for stoichiometric calculations it was considered to be nitrate. Given the relation between nitrogen and organic matter performance, especially in the denitrification process, the later one was included in the model.

Table 1. Description of the components included in the model.

Components	Description	Units
1. S_{NH4}	Ammonium concentration.	mg N L^{-1}
2. S_{NO3}	Nitrate concentration.	mg N L^{-1}
3. S_s	Reactive soluble organic matter concentration.	mg COD L^{-1}
4. S_i	Inert soluble organic matter concentration.	mg COD L^{-1}
5. X_s	Reactive particulate organic matter concentration.	mg COD L^{-1}
6. X_i	Inert particulate organic matter concentration.	mg COD L^{-1}
7. X_H	Heterotrophic microorganisms concentration.	mg COD L^{-1}
8. X_A	Autotrophic microorganisms concentration.	mg COD L^{-1}
9. X_{ml}	Living macrophyte biomass.	g COD m^{-2}
10. X_{md}	Dead standing macrophyte biomass.	g COD m^{-2}

Organic nitrogen (ON), TN, COD_S and COD_T were obtained by adding the nitrogen or the organic matter content of the corresponding components (Eq. 1 to Eq. 4), where i_{NXs}, i_{NXi}, i_{NSs} and i_{NSi} (mg N mg COD^{-1}) are nitrogen content in X_S, X_i, S_S and S_i, respectively, X_p (mg Chl *a* L^{-1}) is phytoplankton concentration,

i_{NXp} (mg N mg Chl a^{-1}) is nitrogen content in phytoplankton (X_P) and i_{CODXp} (mg COD mg Chl a^{-1}) refers to organic matter content in phytoplankton.

$$ON = i_{NXs} \cdot X_s + i_{NXi} \cdot X_i + i_{NSs} \cdot S_s + i_{NSi} \cdot S_i \quad \text{Eq. 1}$$

$$TN = S_{NH4} + S_{NO3} + ON + i_{NXp} \cdot X_P \quad \text{Eq. 2}$$

$$COD_S = S_s + S_i + 4.57 \cdot S_{NO3} \quad \text{Eq. 3}$$

$$COD_T = COD_s + X_s + X_i + X_p \cdot i_{CODXp} \quad \text{Eq. 4}$$

The model proposed simulates the hydrolysis of the reactive particulate organic matter (X_s) by means of heterotrophic microorganisms in both aerobic and anoxic conditions. Hydrolysis produces soluble reactive and inert organic matter (S_s and S_i) as well as ammonium, which is taken as nutrient supply by living macrophyte biomass (X_{ml}), phytoplankton (X_P), heterotrophic microorganisms (X_H) and autotrophic microorganisms (X_A) in their growth processes. The growth of X_A generates nitrate that can also be used as nutrient by X_{ml} and X_P, although ammonium is preferred. Nitrate is used as electron acceptor for X_H growth in anoxic conditions, reducing it to N_2 gas, which is not included in the model. Lysis of X_H and X_A, decay and respiration of X_P and degradation of dead standing macrophyte biomass (X_{md}) recycle ammonium and organic matter to the water column. On the other hand, interactions between water column and sediment layer are included through sedimentation processes of X_s and X_i, resuspension of nitrogen and organic matter content in sediments and diffusion of ammonium and nitrate. Sedimentation and resuspension processes are modelled following Gargallo et al. (2016).

The preferential consumption of ammonium instead of nitrate by X_P was modelled using the preferential factor FP_{NH4} by Thomann and Fitzpatrick (1982) (Eq. 5), where k_{mN} is the saturation coefficient for ammonium. In macrophyte uptake, it was introduced as an inhibition function for ammonium in the nitrate uptake by plant (Rousseau, 2005). Uptake processes by macrophytes were simulated by adapting the first order rate processes used by Rousseau (2005), which in turn were based on the work of Wynn and Liehr (2001). They were considered to take place only during the growing season (GS) and consequently the step function δ(t,GS) was introduced: δ=1 if t $\in$ GS and δ=0 if t $\notin$ GS, where t is the time. Nutrient uptake by macrophyte was considered to take place in the water column and the interaction between belowground biomass and sediments was not included.

$$FP_{NH4} = S_{NH4} \frac{S_{NO3}}{(k_{mN} + S_{NH4})(k_{mN} + S_{NO3})} + S_{NH4} \frac{k_{mN}}{(S_{NH4} + S_{NO3})(k_{mN} + S_{NO3})} \quad \text{Eq. 5}$$

Volatilization of NH_3 was not included in the model since this process has little significance if the pH is below 9.3, which is the case of FWSCWs. Also in SSFCWs, where pH varies between 7.5 and 8.0, this process is considered to be insignificant (Saeed and Sun, 2012).

Following Gargallo et al. (2016), diffusion processes were modelled by modifying Fick´s first law with the parameter $K_{difused}$, which takes into account porosity and tortuosity for modelling diffusion between water and sediments.

In order to take into account the influence of phosphorus, phytoplankton and total suspended solids (X_{TSS}), these variables were modelled according to the model developed by Gargallo et al. (2016). Matrix notation of the model for simulating nitrogen forms, organic matter as well as phytoplankton, phosphorus and total suspended solids is showed in Table 2, kinetic rates are presented in Table 3 and stoichiometric coefficients in Table 4. Processes 1 to 14 are newly developed in this study, whereas processes 15-24 are adapted from Gargallo et al. (2016). Apart from processes included in Table 2, resuspension by wind was modelled as Gargallo et al. (2016) in order to simulate resuspension of nitrogen and organic matter content in sediments.

Processes 15 to 24 were modelled using the kinetic expressions by Gargallo et al. (2016), whereas the growth of phytoplankton was modified by including the Monod expression for the dissolved inorganic nitrogen, DIN, which is formed by the sum of ammonium and nitrate.

Temperature influence was modelled using the modified Arrhenius Eq. 6:

$$K_T = K_{20}\theta^{T-20} \qquad \text{Eq. 6}$$

where K_T (d^{-1}) is the value of the kinetic parameter at a certain temperature T, K_{20} (d^{-1}) is the value of the kinetic parameter at 20ºC, θ stands for the coefficient of correction for temperature and T (ºC) is operating temperature.

Table 2. Stoichiometric matrix of the model. Grey colour indicates processes adapted from Gargallo et al. (2016). The sub index *bm* refers to microorganisms composition.

Component → Process ↓	TIP	P_{int}	S_{NH4}	S_{NO3}	S_s	S_i	X_P	X_H	X_A	X_S	X_i	X_{ml}	X_{md}	X_{TSS}
1. Hydrolysis	U_{1TIP}		U_{1NH4}		1- $f_{hyd,Si}$	$f_{hyd,Si}$				-1				
2. Anoxic hydrolysis	U_{2TIP}		U_{2NH4}		1- $f_{hyd,Si}$	$f_{hyd,Si}$				-1				
3. Aerobic growth of X_H	$-i_{Pbm}$ $+i_{PSs}/Y_H$		$-i_{Nbm}+i_{NSs}/Y_H$		$-1/Y_H$			1						
4. Anoxic growth of X_H	$-i_{Pbm}$ $+i_{PSs}/Y_H$		$-i_{Nbm}+i_{NSs}/Y_H$	$-(1-Y_H)/(2.86Y_H)$	$-1/Y_H$			1						
5. Lysis de X_H	U_{5TIP}		U_{5NH4}		$f_{bm,Ss}$			-1		U_{5Xs}	$f_{bm,Xi}$			
6. Growth of X_A	$-i_{Pbm}$		$-i_{Nbm}-1/Y_A$	$1/Y_A$					1					
7. Lysis de X_A	U_{7TIP}		U_{7NH4}		$f_{bm,Ss}$				-1	U_{7Xs}	$f_{bm,Xi}$			
8. S_{NH4} uptake by X_{ml}	$-i_{PXm}$		$-i_{NXm}$									1		
9. S_{NO3} uptake by X_{ml}	$-i_{PXm}$			$-i_{NXm}$								1		
10. X_{md} degradation	U_{10TIP}		U_{10NH4}							1- f_{plant}	f_{plant}		-1	
11. Diffusion of S_{NH4}			1											
12. Diffusion of S_{NO3}				1										
13. Sedimentation of X_S										-1				
14. Sedimentation of X_i											-1			
15. Phosphorus uptake by X_P	$-X_P$	1												
16. Growth of X_P		$-i_{PXp}/X_P$	$-FP_{NH4}\cdot i_{NXp}$	$-(1-FP_{NH4})\cdot i_{NXp}$			1							i_{TSSXp}
17. Decay of X_P	U_{17TIP}		U_{17NH4}		$f_{XpSs}\cdot i_{CODXp}$		-1			U_{17Xs}	$f_{XpXi}\cdot i_{CODXp}$			$-i_{TSSXp}$
18. Lysis of P_{int}	X_P	-1												
19. Respiration of X_p	U_{19TIP}		U_{19NH4}		$f_{XpSs}\cdot i_{CODXp}$		-1			U_{19Xs}	$f_{XpXi}\cdot i_{CODXp}$			$-i_{TSSXp}$
20. Sedimentation of X_P							-1							$-i_{TSSXp}$
21. Sedimentation of PIP	-1													
22. Diffusion of DIP	1													
23. Sedimentation of X_{SST}														-1
24. Resuspension by avifauna										i_{CODsed}				1

200 Table 3. Processes kinetics.

Process	Process rate
1. Hydrolysis	$r_1 = k_h \cdot \theta_{kh}^{T-20} \frac{X_s/X_H}{k_x + X_s/X_H} \frac{DO}{K_{hyd\ DO} + DO} X_H$
2. Anoxic hydrolysis	$r_2 = k_h \cdot O_h \cdot \theta_{kh}^{T-20} \frac{X_s/X_H}{k_x + X_s/X_H} \frac{K_{hyd\ DO}}{K_{hyd\ DO} + DO} \frac{S_{NO3}}{k_{NOH} + S_{NO3}} X_H$
3. Aerobic growth X_H	$r_3 = \mu_H \cdot \theta_{\mu H}^{T-20} \frac{S_s}{K_s + S_s} \frac{DO}{K_{OH} + DO} \frac{S_{NH4}}{K_{NHH} + S_{NH4}} \frac{TIP \cdot f_d}{K_{PH} + TIP \cdot f_d} X_H$
4. Anoxic growth X_H	$r_4 = \eta_{NO3} \cdot \mu_H \cdot \theta_{\mu H}^{T-20} \frac{S_s}{K_s + S_s} \frac{K_{OH}}{K_{OH} + DO} \frac{S_{NO3}}{K_{NOH} + S_{NO3}} \frac{S_{NH4}}{K_{NHH} + S_{NH4}} \frac{TIP \cdot f_d}{K_{PH} + TIP \cdot f_d} X_H$
5. Lysis of X_H	$r_5 = b_H \cdot \theta_{bH}^{T-20} \cdot X_H$
6. Growth of X_A	$r_6 = \mu_A \cdot \theta_{\mu A}^{T-20} \frac{S_{NH4}}{K_{NHA} + S_{NH4}} \frac{DO}{K_{OA} + DO} \frac{TIP \cdot f_d}{K_{PA} + TIP \cdot f_d} X_A$
7. Lysis of X_A	$r_7 = b_A \cdot \theta_{bA}^{T-20} \cdot X_A$
8. Diffusion of S_{NH4}	$r_8 = Do_{NH4} \cdot \theta_{d\ NH4}^{T-20} \cdot (NH4_{sed} - S_{NH4}) \cdot \frac{A}{0.1 \cdot V}$
9. Diffusion of S_{NO3}	$r_9 = Do_{NO3} \cdot \theta_{d\ NO3}^{T-20} \cdot (NO3_{sed} - S_{NO3}) \cdot \frac{A}{0.1 \cdot V}$
10. Sedimentation of X_S	$r_{10} = \frac{vs_X}{H} \cdot (1 + VC \cdot K_{veg\ sed}) \cdot X_S$
11. Sedimentation of X_I	$r_{11} = \frac{vs_X}{H} \cdot (1 + VC \cdot K_{veg\ sed}) \cdot X_i$
12. S_{NH4} uptake by X_{ml}	$r_{12} = \frac{1}{H} \cdot K_{pl} \cdot \theta_{up\ plant}^{T-20} \frac{S_{NH4}}{K_{NHP} + S_{NH4}} \frac{TIP \cdot f_d}{K_{PP} + TIP \cdot f_d} X_{ml} \cdot \delta(t, GS)$
13. S_{NO3} uptake by X_{ml}	$r_{13} = \frac{1}{H} \cdot K_{pl} \cdot \theta_{up\ plant}^{T-20} \frac{S_{NO3}}{K_{NOP} + S_{NO3}} \frac{K_{NHP}}{K_{NHP} + S_{NH4}} \frac{TIP \cdot f_d}{K_{PP} + TIP \cdot f_d} X_{ml} \cdot \delta(t, GS)$
14. Plant degradation	$r_{14} = \frac{1}{H} \cdot K_{deg} \cdot \theta_{deg}^{T-20} \cdot X_{md}$

201

202 Table 4. Stoichiometric coefficients.

$$\upsilon_{1TIP} = \upsilon_{2TIP} = i_{PXs} - f_{hyd,Si} \cdot i_{PSi} - (1 - f_{hyd,Si}) \cdot i_{PSs}$$

$$\upsilon_{1NH4} = \upsilon_{2NH4} = i_{NXs} - f_{hyd,Si} \cdot i_{NSi} - (1 - f_{hyd,Si}) \cdot i_{NSs}$$

$$\upsilon_{5TIP} = \upsilon_{7TIP} = i_{Pbm} - f_{bmSs} \cdot i_{PSs} - i_{PXs} \cdot (1 - f_{bmSs} - f_{bmXi}) - i_{PXi} \cdot f_{bmXi}$$

$$\upsilon_{5NH4} = \upsilon_{7NH4} = i_{Nbm} - f_{bmSs} \cdot i_{NSs} - i_{NXs} \cdot (1 - f_{bmSs} - f_{bmXi}) - i_{NXi} \cdot f_{bmXi}$$

$$\upsilon_{5Xs} = \upsilon_{7Xs} = 1 - f_{bmSs} - f_{bmXi}$$

$$\upsilon_{10TIP} = i_{PXm} - f_{plant} \cdot i_{PXi} - (1 - f_{plant}) \cdot i_{PXs}$$

$$\upsilon_{10NH4} = i_{NXm} - f_{plant} \cdot i_{NXi} - (1 - f_{plant}) \cdot i_{NXs}$$

$$\upsilon_{17TIP} = \upsilon_{19TIP} = i_{PXp} - f_{XpSs} \cdot i_{CODXp} \cdot i_{PSs} - (i_{CODXp}(1 - f_{XpSs} - f_{XpXi})) \cdot i_{PXs} - f_{XpXi} \cdot i_{CODXp} \cdot i_{PXi}$$

$$\upsilon_{17NH4} = \upsilon_{19NH4} = i_{NXp} - f_{XpSs} \cdot i_{CODXp} \cdot i_{NSs} - (i_{CODXp}(1 - f_{XpSs} - f_{XpXi})) \cdot i_{NXs} - f_{XpXi} \cdot i_{CODXp} \cdot i_{NXi}$$

$$\upsilon_{17Xs} = \upsilon_{19Xs} = i_{CODXp} \cdot (1 - f_{XpSs} - f_{XpXi})$$

2.3 Calibration and validation procedures

Data collected in the set of FWSCWs in *Tancat de la Pipa* were used to calibrate and validate the model stated. Calibration was carried out in the FWSCW named as FG1 by adjusting parameter values in order to obtain the best fit between simulated and observed data (April 2009-April 2012). Afterwards, the model was validated using the data from the FWSCW FG2.

The model developed was implemented in the software AQUASIM (Reichert, 1994), which uses the variable-order Gear integration technique to solve differential equations (Reichert, 1998). Processes reactions were introduced as dynamic processes, components as state variables and the rest of parameters as programme, constant, real list or formula variables. The mixed reactor compartment configuration was used and defined by the volume of the wetland, active variables, active processes, initial conditions and inputs. Hydraulic performance of the systems FG1 and FG2 was simulated such as in Gargallo et al. (2016) by applying a mass balance.

Table 5. Initial conditions for the component concentrations in FWSCWs FG1 and FG2.

Component	Units	Initial conditions	
		FG1(calibration)	FG2 (validation)
S_{NH4}	mg N L^{-1}	0.134	0.005
S_{NO3}	mg N L^{-1}	0.848	0.018
S_s	mg COD L^{-1}	4.82	4.96
S_i	mg COD L^{-1}	19.28	19.84
X_s	mg COD L^{-1}	3.87	4.4
X_i	mg COD L^{-1}	0.53	0.6
X_H	mg COD L^{-1}	0.001	0.001
X_A	mg COD L^{-1}	0.001	0.001
X_{ml}	g COD m^{-2}	505.4	505.4
X_{md}	g COD m^{-2}	0.005	0.005
TIP	mg P L^{-1}	0.421	0.093
P_{int}	mg P mg Chl *a* $^{-1}$	0.52	0.52
X_P	mg Chl *a* L^{-1}	0.007	0.001
X_{SST}	mg L^{-1}	16.5	10.1

Initial conditions were set to the concentrations measured in the outflow of the systems during the first sampling campaign (Table 5). Initial concentrations of both autotrophic and heterotrophic microorganisms were established in 0.001 mg COD L^{-1} in order to recreate the start-up situation and to reduce the impact of imposed initial conditions (Samsó and Garcia, 2013). Microorganisms concentration in inflow water was assumed to be null.

Regarding to macrophyte biomass, living and dead standing macrophyte biomasses were introduced as input data. X_{ml} and X_{md} were calculated from both VC and maximum aboveground biomass reported by Gargallo et al. (2016) and Hernández-

Crespo et al. (2016), respectively, since regular measurements of plant biomass were not available. Provided that FG1 and FG2 presented heterogeneous biomass distribution along their surfaces, it was considered that mean biomass density when the systems were fully vegetated (VC=1) was half the maximum value reported in the abovementioned study (i.e. 0.95 kg dw m^{-2}, where dw means dry weight). Total biomass (X_{ml} + X_{md}) along the studied period was calculated by multiplying this maximum biomass density by the VC and applying the ratio 1.33 g COD g dw^{-1} obtained from the same study (Hernández-Crespo et al., 2016). At the beginning of the studied period, X_{md} was considered to be negligible in both CWs since fresh biomass was planted (Martín et al., 2013). Macrophyte biomass in FG1 was harvested in October 2010 and vegetation did not grow up again so the entire aboveground biomass existing during the studied period was considered to be X_{ml}. On the other hand, FG2 was not harvested and vegetation started to globally decay from March 2010 until the end of the period (Oliver et al., 2016), thus a distribution between X_{ml} and X_{md} was established based on field observations (Figure 1).

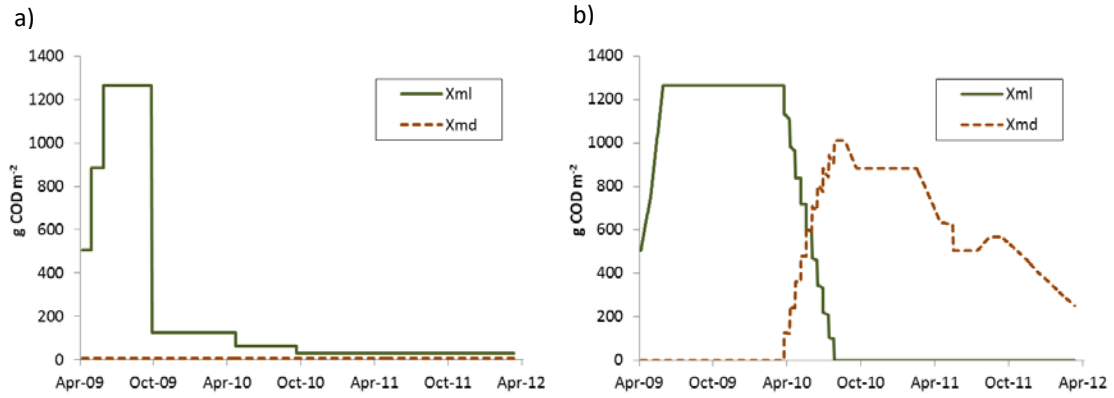

Figure 1. Estimated X_{ml} and X_{md} (g COD m^{-2}) in (a) FG1 and (b) FG2 FWSCWs.

Following the references compiled in Kadlec and Wallace (2009) for *Typha spp.*, the growing season was considered to be from February to mid-September.

Nitrification and denitrification processes, which are respectively modelled by means of the growth of X_A and the anoxic growth of X_H, are inversely affected by DO so they cannot occur at the same time within a completely mixed reactor compartment. In FWSCW these processes can be spatially separated since nitrification mainly occurs in areas where high DO concentrations are registered (e.g. near to water surface or near the rhizosphere) and denitrification takes places in water-sediment interface with lower DO concentrations (Babourina, 2012). Mainly due to phytoplankton photosynthesis and respiration, DO concentrations present notorious oscillations along one day in hypertrophic systems, which mostly depend on phytoplankton concentration, temperature, light intensity and nutrients availability. Since DO is an input variable in the proposed model, their values in the mixed reactor were introduced with a time step of 0.5 days. For each day, one of the values corresponds to diurnal conditions and the other one to nocturnal conditions, with linear

interpolation connecting both points. Diurnal concentrations corresponded to biweekly measured values, which were interpolated between each measurement. Continuous monitoring carried out seasonally was used for assigning minimum observed values as nocturnal DO concentrations: 5.03 mg O_2 L^{-1} in spring, 1.27 mg O_2 L^{-1} in summer, 0.61 mg O_2 L^{-1} in autumn and 3.51 mg O_2 L^{-1} in winter (Figure 2).

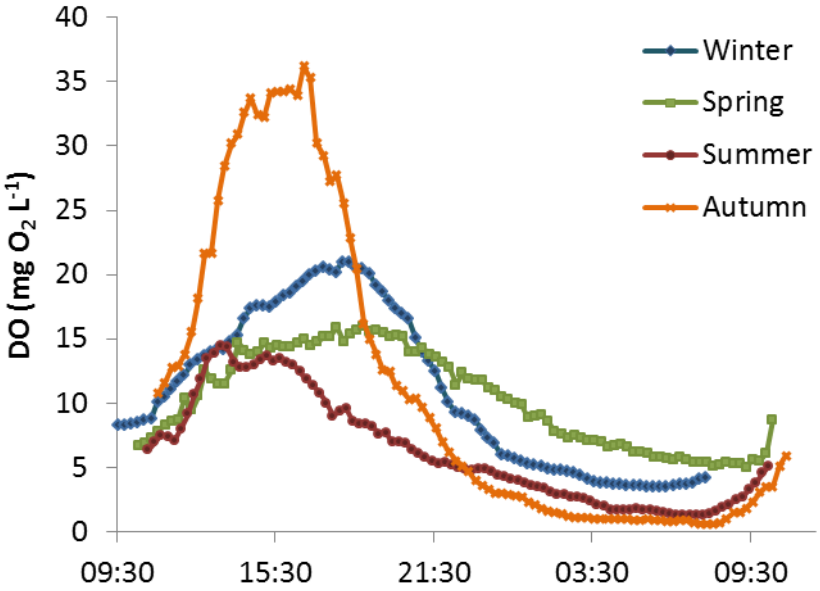

Figure 2. Seasonal daily evolution of DO concentrations in P1.

Values of the parameters used in Gargallo et al. (2016) were kept invariable during the calibration procedure.

The root mean square error (RMSE, Eq. 7) was used to evaluate the adjustment of the model by comparing simulated and observed outlet concentrations:

$$\mathrm{RMSE} = \sqrt{\frac{\sum_{i=1}^{n}(Y_i^{obs} - Y_i^{sim})^2}{n}} \qquad \text{Eq. 7}$$

where Y_i^{obs} and Y_i^{sim} are observed and simulated concentrations, respectively, while *n* is the total number of observations.

2.4 Sensitivity analysis

The parametric sensitivity of the model was studied in order to evaluate the influence of each parameter in the model response. The relative sensitivity (S_x) (Hopkins, 1983) shows the influence of each parameter *k* over each output variable *i* (Eq. 8).

$$S_x = \frac{\Delta i/i}{\Delta k/k} \quad \text{Eq. 8}$$

Mean values of S_X over S_{NH4}, S_{NO3}, TN, COD_T and COD_S during the studied period were calculated in the system FG1 by introducing a variation of ± 10% (Δk = ± 0.1) over the calibration value of each parameter.

3. Results and discussion

3.1 Calibration and validation results

First results obtained by implementing the developed model did not satisfactorily reproduce field measurements. Simulated concentrations were more similar to those measured at the inlet than at the outlet of the studied FWSCWs. For example, in the case of nitrate, which is mainly removed by anoxic growth of X_H, mean concentrations of nitrate measured in P0 and P1 were 2.13 and 0.98 mg N L^{-1}, respectively, whereas mean concentration simulated in P1 was 1.96 mg N L^{-1}. Low average concentrations of X_A and X_H were found in the systems: in FG1, $2 \cdot 10^{-5}$ and 2.85 mg COD L^{-1}, respectively. After carrying out some simulations and discarding important limitations due to the concentrations of substrates (e.g. S_{NH4}, S_S, S_{NO3})that could result in low values in the Monod expressions, it was stated that the mobility imposed to microorganisms (they were modelled as state variables) was generating those poor results. In order to solve this issue, the pattern used in CW2D for subsurface flow CWs (Langergraber and Šimůnek, 2005) was taken into account and microorganisms were considered to be immobile. They were not assumed to be floating in the water column but attached to available surfaces (e.g. surface layer of sediment, lateral banks in the FWSCW or submerged stems of vegetation). Provided that X_A and X_H were included as state variables in the model, an appropriate way to model their immobility feature in the mixed reactor in AQUASIM was to include a theoretical recirculation of microorganisms, considering that the large majority of them (99%) were immobile in the system. Including this assumption was possible because this model does not aim to accurately study the biofilm in FWSCWs but to simulate main trends in nitrogen removal using a process-based model which includes, among other, the response of autotrophic and heterotrophic microorganisms. Taking into account the immobility feature of the microorganisms, the mean nitrate concentration simulated in P1 was 1.03 mg N L^{-1}, which is close to mean measured concentration. Mean simulated concentrations of X_A and X_H in FG1 increased to 0.76 and 107 mg COD L^{-1}, respectively, considering immobility feature.

Other models such as Llorens et al. (2011) consider the mobility of microorganisms in CWs and include bacteria input in the inflow. However, the recirculation approach

presents the advantage that microorganisms remain in the system and the influence of growth and lysis processes can be studied.

On the other hand, an enhancement was needed in order to improve nitrate and organic matter simulation in FG1, where high values of RMSE were initially obtained (2.8 mg N L^{-1} for nitrate, 17.7 mg L^{-1} for COD_T and 12.06 mg L^{-1} for COD_S). It was stated that the lowest value for Monod expression during the studied period was obtained for S_S (mean value of Monod expression for S_S was 0.28, 0.90 for S_{NO3}, 0.66 for S_{NH4} and 0.86 for DIP). However, after some simulations, it was observed that nitrate and organic matter concentrations were better simulated when Monod expression for S_S was fixed to 1. This value for organic matter limitation could be assumed because anoxic growth of X_H takes place in the water sediment interface, where low DO concentrations occur and high organic matter accumulations were observed in this part of the system FG1. The results obtained by including this consideration better adjusted to observed data, especially for nitrate concentrations (RMSE for S_{NO3} was 1.09 mg N L^{-1}, for COD_T was 15.9 mg L^{-1} and for COD_S was 7.6 mg L^{-1}), and they suggest that organic matter needed for anoxic growth of X_H in system FG1 was supplied from these accumulations.

However, S_{NO3}, COD_T and COD_S were properly simulated in FG2 using Monod expression for S_S (RMSE were 0.57 mg N L^{-1}, 12.9 mg L^{-1} and 8.1 mg L^{-1}, respectively) and the saturation coefficient for S_S (k_S) was calibrated to 0.005 mg COD L^{-1}. It means that limitation related to S_S in the anoxic growth of X_H was weaker in FG2 because organic matter accumulations in this system were much smaller than in FG1 and therefore less S_S was supplied by this source.

Hereafter, the comparison between observed and simulated data for measured variables in FG1 and FG2 systems, including the abovementioned considerations, are presented (i.e. ammonium, nitrate, ON, TN, COD_T and COD_S).

Figure 3 and Figure 4 show that the model was successfully calibrated and validated since the main trends of nitrogen forms and organic matter concentrations observed in both FWSCWs were properly simulated.

Ammonium performance is well represented, showing better fitting when values are low. Furthermore, the model properly simulates the observed capacity of these FWSCWs for reducing ammonium peaks entering to the system. Despite the RMSE is high when comparing with mean inlet concentrations (Table 6), mean outlet observed and simulated concentrations are quite similar. Nitrate concentrations are successfully simulated in both systems.

ON and TN simulations, which were calculated using Eq. 1 and Eq. 2, presented different performances. ON was successfully simulated in calibration and validation procedures (RMSE = 0.07 and 0.05 mg N L^{-1}, respectively), whereas modelled TN concentrations were significantly lower than observed ones.

354 Regarding organic matter, the best results were obtained for COD_S (RMSE = 7.6 and
355 8.1 mg L^{-1}, respectively). Conversely, the poorest fitting was obtained for COD_T in
356 FG1 and it could be due to the aforementioned large amount of particulate organic
357 matter accumulated in the bottom of this system.

358

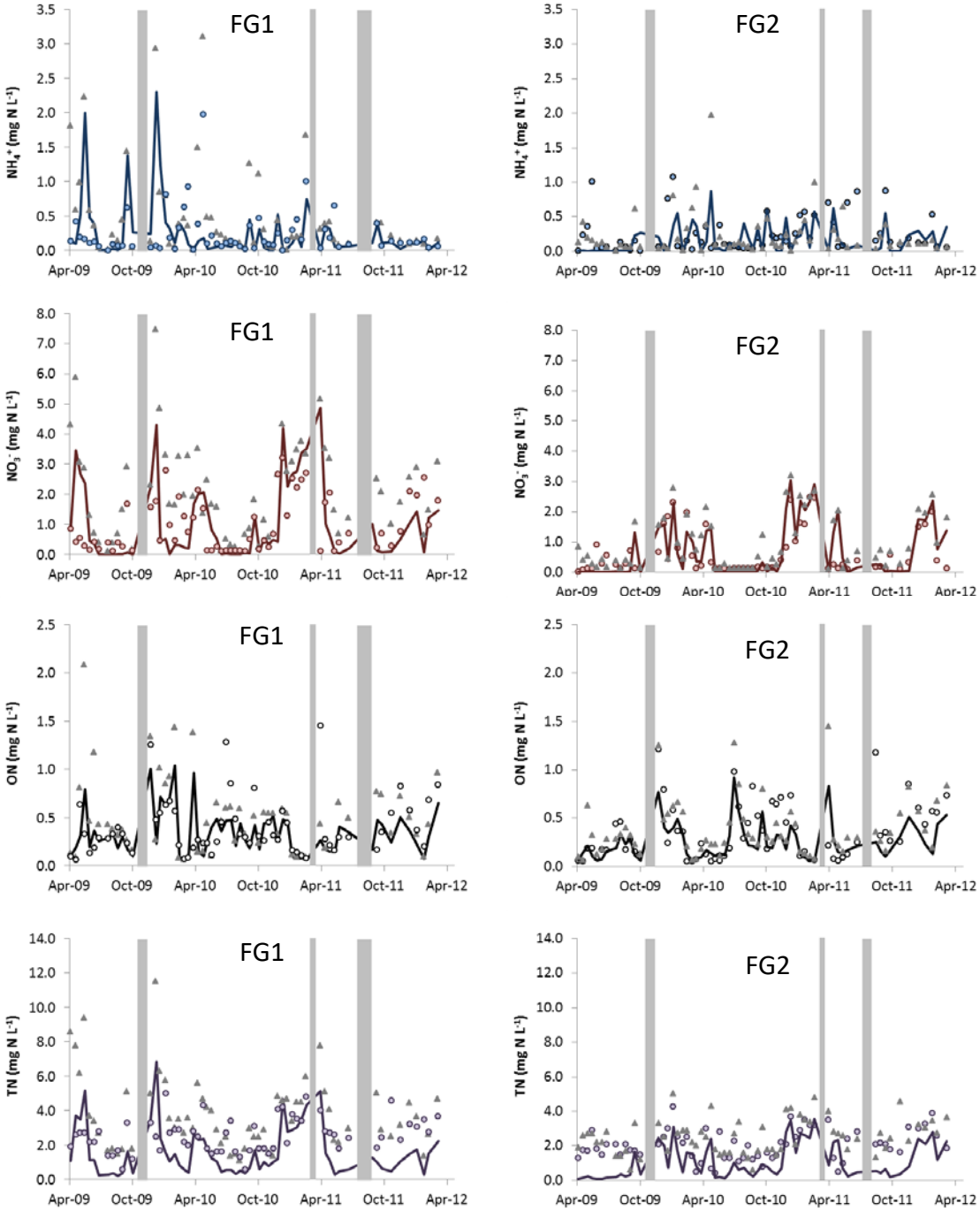

359

360 Figure 3. Temporal evolution of observed and simulated ammonium, nitrate, ON and TN
361 concentrations in FG1 and FG2 FWSCWs. Triangles represent inlet concentrations, circles observed
362 outlet concentrations and line simulated concentrations. Grey bars indicate dried periods in the CWs.

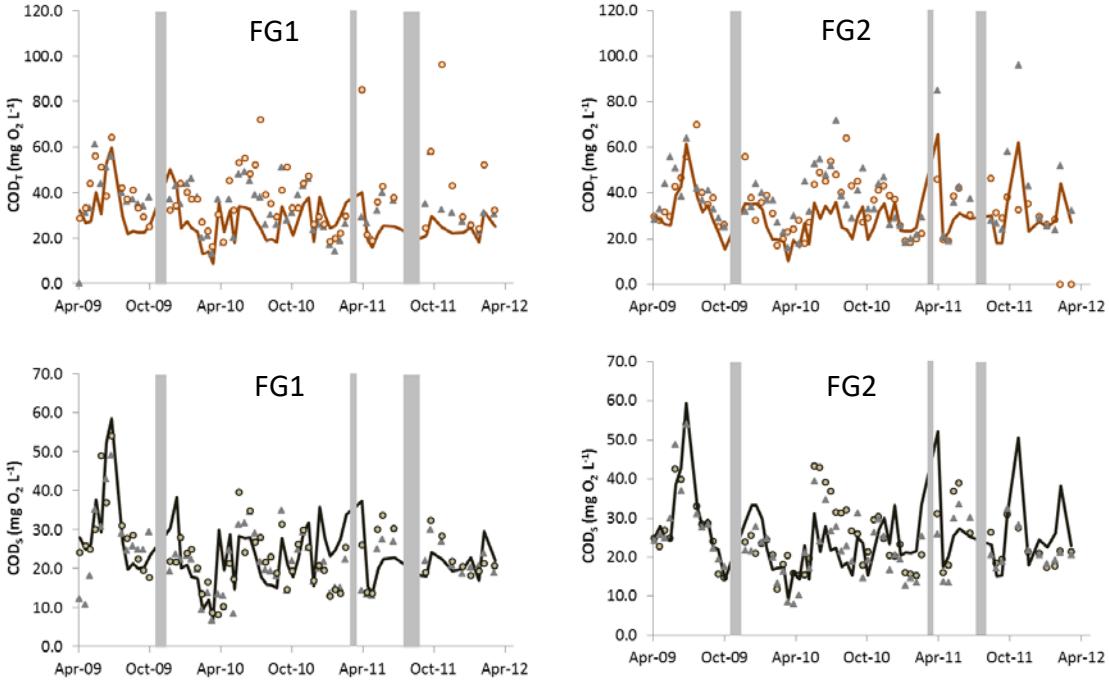

Figure 4. Temporal evolution of observed and simulated COD_T and COD_S concentrations in FG1 and FG2 FWSCWs. Triangles represent inlet concentrations, circles observed outlet concentrations and line simulated concentrations. Grey bars indicate dried periods in the CWs.

Table 6. Mean observed and simulated concentrations and RMSE obtained in calibration and validation procedures.

	Ammonium (mg N L^{-1})	Nitrate (mg N L^{-1})	ON (mg N L^{-1})	TN (mg N L^{-1})	COD_T (mg COD L^{-1})	COD_S (mg COD L^{-1})
FG1 (calibration)						
Mean inlet observed concentration	0.490	2.13	0.49	3.8	33.2	22.2
Mean outlet observed concentration	0.233	0.98	0.09	2.6	38.0	23.4
Mean outlet simulated concentration	0.286	1.03	0.03	1.7	32.1	23.8
RMSE	**0.556**	**1.09**	**0.07**	**1.6**	**15.9**	**7.6**
FG2 (validation)						
Mean inlet observed concentration	0.230	0.97	0.09	2.5	37.8	23.4
Mean outlet observed concentration	0.240	0.62	0.07	2.1	35.1	25.1
Mean outlet simulated concentration	0.194	0.71	0.04	1.2	28.1	24.3
RMSE	**0.330**	**0.57**	**0.05**	**1.3**	**12.9**	**8.1**

The parameter values obtained in the calibration procedure are shown in Table 7 and Table 8. The maximum growth velocity of heterotrophic microorganisms obtained by

Mcbride and Tanner (2000) for modelling nitrogen removal in SSFCWs with water level fluctuations was used, which is slightly lower than the value of 6 d^{-1} commonly used in SSFCWs models (Langergraber et al., 2009; Langergraber and Šimůnek, 2005; Mburu et al., 2012; Samsó and Garcia, 2013).

Regarding μ_A, the calibrated value was very similar to the growth velocity of second stage nitrifier microorganisms set by Reichert et al. (2001) (1.1 d^{-1}), presenting an intermediate value between the 1 d^{-1} commonly used in CWM1, CW2D or BIO-pore and the value of 1.5 d^{-1} set by Pálfy and Langergraber (2014).

Table 7. Stoichiometric parameters.

Parameter	Description	Value	Source
Phytoplankton			
K_{mN}	Saturation coefficient for S_{NH4} (mg N L^{-1})	0.025	(1)
Hydrolysis			
k_h	Hydrolysis rate constant (d^{-1})	3	(2)
O_h	Anoxic hydrolysis reduction factor	0.6	(2)
$K_{hyd\ DO}$	Saturation/inhibition coefficient for oxygen (mg O_2 L^{-1})	0.2	(2)
k_x	Saturation/inhibition coefficient for hydrolysis (mg COD_S mg COD_{bm}^{-1})	0.1	(2)
Heterotrophic bacteria			
μ_H	Maximum aerobic growth rate (d^{-1})	5	(3)
b_H	Rate constant for lysis (d^{-1})	0.4	(2)
η_{NO3}	Correction factor for denitrification	0.8	(2)
K_{NHH}	Saturation coefficient for S_{NH4} (mg N L^{-1})	0.05	(2)
K_{NOH}	Saturation/inhibition coefficient for S_{NO3} (mg N L^{-1})	0.05	This study
K_S	Saturation coefficient for S_S (mg COD L^{-1})	0.005	This study
K_{OH}	Saturation/inhibition coefficient for DO (mg O_2 L^{-1})	0.5	This study
K_{PH}	Saturation/inhibition coefficient for DIP (mg P L^{-1}).	0.001	This study
$\theta_{\mu H}$	Temperature coefficient for growth	1.0718	(2)
θ_{bH}	Temperature coefficient for lysis	1.0718	(2)
θ_{Kh}	Temperature coefficient for hydrolysis	1.014	(2)
Autotrophic bacteria			
μ_A	Maximum growth rate (d^{-1})	1.2	This study
b_A	Rate constant for lysis (d^{-1})	0.15	(2)
K_{NHA}	Saturation coefficient for S_{NH4} (mg N L^{-1})	0.4	This study
K_{OA}	Saturation coefficient for DO (mg O_2 L^{-1})	1	(4)
$\theta_{\mu A}$	Temperature coefficient for growth	1.1107	(2)
θ_{bA}	Temperature coefficient for lysis	1.1161	(2)
Interaction with sediment layer			
v_{sX}	Sedimentation rate of X_s and X_i (m d^{-1})	0.03	This study
Do_{NH4}	Diffusion coefficient for S_{NH4} (m^2 d^{-1})	$1.71 \cdot 10^{-4}$	(5)
Do_{NO3}	Diffusion coefficient for S_{NO3} (m^2 d^{-1})	$1.64 \cdot 10^{-4}$	(5)
$\theta_{difu\ NH4}$	Temperature coefficient for S_{NH4} diffusion	1.0237	(5)
$\theta_{difu\ NO3}$	Temperature coefficient for S_{NO3} diffusion	1.0239	(5)
Plants			
K_{pl}	Plant growth rate (d^{-1})	0.028	(6)
K_{deg}	Plant degradation rate (d^{-1})	0.0025	This study
K_{NHP}	Saturation/inhibition coefficient for S_{NH4} (mg N L^{-1})	0.1	This study
K_{NOP}	Saturation coefficient for S_{NO3} (mg N L^{-1})	0.1	(7)
k_{PP}	Saturation coefficient for DIP (mg P L^{-1}).	0.0005	This study
$\theta_{up\ plant}$	Temperature coefficient for plant uptake	1.09	(8)
θ_{deg}	Temperature coefficient for plant degradation	1.0524	(9)

(1): Ambrose et al. (1988); (2): Henze et al. (2000); (3): Mcbride and Tanner (2000); (4): Langergraber and Šimůnek (2005); (5): Reddy and DeLaune (2008); (6): Hernández-Crespo et al. (2016); (7): Kadlec and Knight (1996); (8): Asaeda and Karunaratne (2000); (9): Álvarez and Bécares (2006).

Many saturation/inhibition coefficients were lower than those commonly used for treating domestic wastewater (Henze et al., 2000; Langergraber et al., 2009; Langergraber and Šimůnek, 2005; Samsó and Garcia, 2013) because hypertrophic

water treated in FWSCWs FG1 and FG2 presented lower ammonium, nitrate and organic matter concentrations than domestic wastewater and lower saturation/inhibition coefficients were obtained for these variables. However, DO oscillations registered in the system provided higher inhibition/saturation coefficient for oxygen.

Nitrogen content in X_p (i_{NXp}) was calculated by applying the Redfield mass ratio to the phytoplankton composition obtained in Gargallo et al. (2016), whereas phosphorus content in phytoplankton entering to FG1 was set to 1.04 mg P mg Chl a^{-1}.

Regarding macrophyte composition, nitrogen content measured by Hernández-Crespo et al. (2016) was used, which was lower than the value obtained by Romero et al. (1999) for *Phragmites australis*. This low content of nitrogen forced to fix lower nitrogen content, both in microorganisms and in organic matter forms than those usually used in order to accomplish mass balances. The plant growth rate set by Hernández-Crespo et al. (2016) was used and the calibrated plant degradation rate (K_{deg}=0.0025 d^{-1}) was very similar to the value of 0.0020 d^{-1} presented by Álvarez and Bécares (2006).

Ammonium and nitrate concentrations in pore water in sediments were set to concentrations measured by Hernández-Crespo (2013) in sediments from Lake Albufera ($NH4_{sed}$ = 55 mg N L^{-1} and $NO3_{sed}$ = 0.4 mg N L^{-1}, respectively).

Table 8. Composition parameters.

Parameter	Description	Value	Source
Y_H	Yield coefficient for X_H (mg COD_{bm} mg COD S_S^{-1})	0.63	(2)
Y_A	Yield coefficient for X_A (mg COD_{bm} mg N^{-1})	0.24	(2)
f_{XpSs}	Fraction of S_S generated in X_p decay and respiration (mg COD_{Ss} mg COD_{Xp}^{-1})	0.1	This study
f_{XpXi}	Fraction of X_i generated in X_p decay and respiration (mg COD_{Xi} mg COD_{Xp}^{-1})	0.01	This study
f_{bmSs}	Fraction of S_S generated in microorganisms lysis (mg COD_{Ss} mg COD_{bm}^{-1})	0.1	This study
f_{bmXi}	Fraction of X_i generated in microorganisms lysis (mg COD_{Ss} mg COD_{bm}^{-1})	0.01	This study
$f_{hyd,Si}$	Fraction of X_i generated in hydrolysis (mg COD_{Si} mg COD_{Xs}^{-1})	0	(2)
f_{plant}	Fraction of X_i generated in plant degradation (mg COD_{Xi} mg COD_{Xmd}^{-1})	0.2	(10)
i_{NXp}	N content of X_p (mg N mg Chl a^{-1})	7.52	This study
i_{CODXP}	COD content of X_p (mg COD mg Chl a^{-1})	114.01	This study
i_{Nbm}	N content of microorganisms (mg N mg CDO_{bm}^{-1})	0.07	(2)
i_{Pbm}	P content of microorganisms (mg P mg COD_{bm}^{-1})	0.01	This study
i_{NXm}	N content of microorganisms (mg N mg COD_{bm}^{-1})	0.07	(6)
i_{NSs}	N content of S_S (mg N mg COD_{Ss}^{-1})	0.003	This study
i_{NSi}	N content of S_i (mg N mg COD_{Si}^{-1})	0.001	This study
i_{NXs}	N content of X_s (mg N mg COD_{Xs}^{-1})	0.004	This study
i_{NXi}	N content of X_i (mg N mg COD_{Xi}^{-1})	0.003	This study
i_{PSs}	P content of S_S (mg P mg DQO^{-1})	0.001	This study
i_{Psi}	P content of S_i (mg P mg DQO^{-1})	0.000	This study
i_{PXs}	P content of X_s (mg P mg DQO^{-1})	0.001	This study
i_{PXi}	P content of X_i (mg P mg DQO^{-1})	0.001	This study
i_{CODsed}	COD content of sediments (mg COD mg TSS^{-1})	0.07	This study

(10): Rousseau (2005).

The influence of alkalinity on the growth of X_A was studied by applying the Monod expression to the measurements carried out in points P0, P1 and P2 and using the value of 0.5 mole HCO_3^- m^{-3} for the saturation coefficient (Henze et al., 2000). The Monod expression for alkalinity presented a mean value of 0.84 for the three studied

points and the minimum value was 0.76. These results suggested that alkalinity was not exerting a substantial limitation in the growth of X_A.

The model properly represents the accumulated removed masses of ammonium and nitrate in FWSCWs over time. Figure 5 and Figure 6 show the case of ammonium and nitrate during the studied period. It can be seen the goodness-of-fit between observed and simulated values in FG1, where the mean error is lower than 10%. The adjustment in FG2 is more adequate until January 2011 and from then on the model overestimates ammonium removal and underestimates nitrate removal. The main hypothesis is that it was produced by the decomposition of the stems cut by the herbivorous bird *Porphyrio porphyrio* (Gargallo et al., 2016; Hernández-Crespo et al., 2016), which released ammonium in the water column and this contribution was not modelled.

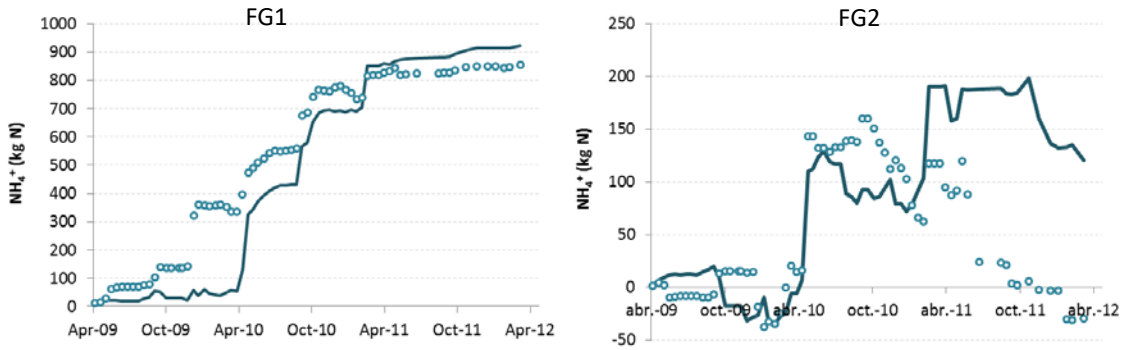

Figure 5. Accumulated mass of removed ammonium in FG1 and FG2. Points represent observed data and line simulated data.

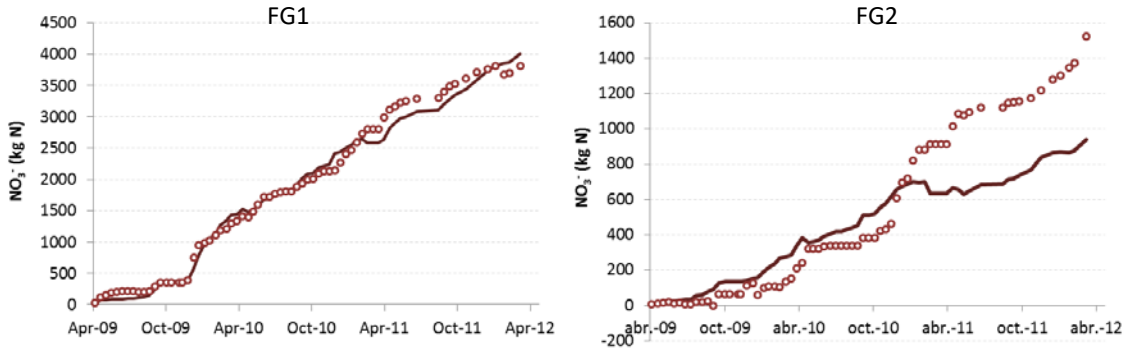

Figure 6. Accumulated mass of removed nitrate in FG1 and FG2. Points represent observed data and line simulated data.

3.2 Mass budgets for nitrogen removal

Pathways for ammonium and nitrate removal were studied in order to highlight the main removal mechanisms in FWSCWs. The influence of each process was calculated in reference to the sum of all the masses entering with influent and internally recycled by the simulated processes in the model.

In both FG1 and FG2 FWSCWs, ammonium was mainly removed by the growth of X_A (Figure 7). In FG2 the contribution of this process was smaller in favour of the processes of heterotrophic microorganisms and plants. According to Oliver et al. (2016), the higher the VC, the higher the ammonium uptake by macrophytes, accounting 9% of the ammonium entering to FG1 and 19% to FG2.

In the balance of ammonium, the mass consumed by the aerobic and anoxic processes of growth as well as the mass recycled in the lysis of X_H were counted as a single value. It represents 12% and 17% of the ammonium in FG1 and FG2, respectively, which is in accordance with the observations by Saeed and Sun (2012). The growth of X_P consumes less than 2% of the ammonium in the system.

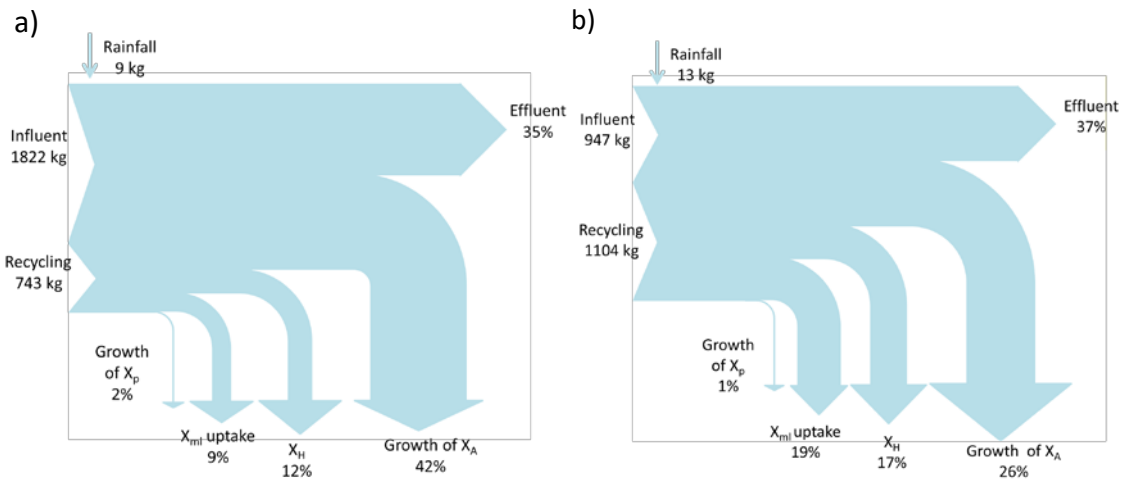

Figure 7. Budget of ammonium removal mechanisms in (a) FG1 and (b) FG2.

The amount of ammonium recycled by internal processes is higher in FG2 and the most contributing processes are diffusion, aerobic hydrolysis, decay and respiration of X_P (Figure 8). The ammonium recycled by macrophyte degradation is negligible in FG1 because vegetation was harvested after the first year of operation, before the senescence of the vegetation; however, it plays an important role in FG2 and adds 8% of the recycled ammonium. Therefore, the importance of vegetation harvesting was confirmed.

In both systems, anoxic hydrolysis and lysis of microorganisms represent less than 5% of recycled ammonium.

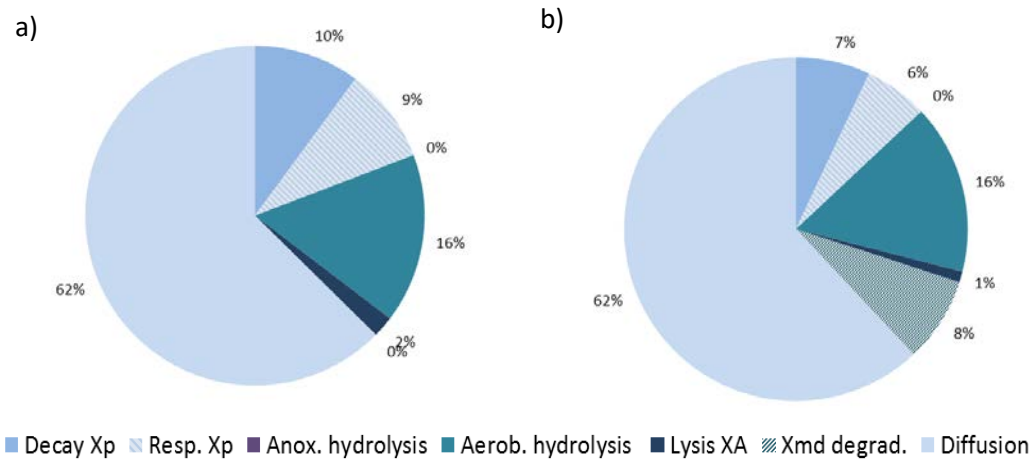

Figure 8. Budget of processes involved in ammonium recycling in (a) FG1 and (b) FG2.

Regarding nitrate performance, it is mainly removed the anoxic growth of X_H (Figure 9), which is consistent with the general assumption that denitrification is one of the most important mechanisms for nitrate removal in constructed wetlands (Garcia et al., 2010; Saeed and Sun, 2012; Sánchez-Carrillo et al., 2011). Nitrate removal by macrophyte uptake was lower than 5% in both systems. Internally recycled nitrate represents 11% of the amount entering to both systems and it is fully produced by the growth of X_A.

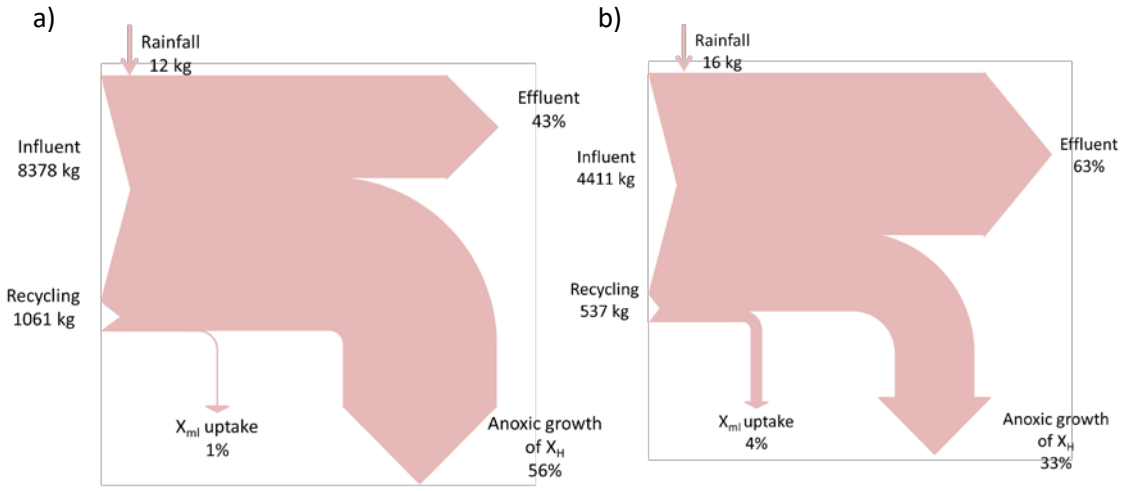

Figure 9. Budget of nitrate removal mechanisms in (a) FG1 and (b) FG2.

3.3 Sensitivity analysis results

The results obtained in the sensitivity analysis (Table 9) showed that nitrate is the most sensitive component in the model developed, followed by ammonium. Organic matter forms (COD_T and COD_S, calculated by means of Eq. 3 and Eq. 4) are less sensitive to changes in the parameter values. The most influential parameters for the five output variables studied are those related to growth and lysis kinetics of X_A and

X_H. Regarding temperature influence, ammonium is sensitive to temperature coefficient for the growth of X_A and nitrate to temperature coefficient for the growth of both X_A and X_H, whereas TN is influenced by the temperature coefficient for the growth of X_H. On the other hand, saturation coefficient for S_{NH4} and DO for the growth of X_A are influential parameters in both ammonium and nitrate. Furthermore, TN is also sensitive to nitrogen content of X_P. COD_T and COD_S are sensitive to growth and lysis rates of X_H, its yield coefficient and the correction factor for denitrification.

Table 9. Relative sensitivity (S_X) ranking for simulated concentrations in the effluent.

S_X	S_{NH4}	S_{NO3}	TN	COD_T	COD_S
> 1	μ_A	μ_H, η_{NO3}, b_H			
0.5 – 1	$K_{NHA}, b_A, \theta_{\mu A}$	μ_A, K_{NHA}, b_A, Y_H	μ_H, η_{NO3},		
0.1 – 0.5	K_{OA}, b_H, Y_H	$\theta_{\mu A}, K_h, \theta_{\mu H}, K_{OA}$	$b_H, i_{NXp}, Y_H, \theta_{\mu H}$	$\mu_H, b_H, Y_H, \eta_{NO3}$,	$\mu_H, b_H, Y_H, \eta_{NO3}$

These observations are consistent with those carried out in Mburu et al. (2012) where it was stated that parameters with the highest sensitivities were those related to microorganisms kinetics and sorption processes, which were also included in the model CWM1-AQUASIM. Likewise, the results obtained also agree with the analysis carried out by Rousseau (2005) where η_{NO3}, K_{OA}, $\theta_{\mu A}$ and $\theta_{\mu H}$ were demonstrated to be some of the most influential parameters in that model.

4. Conclusions

A process-based model following the structure of ASMs was developed for nitrogen forms simulation in FWSCWs treating eutrophic water. Using the software AQUASIM, it was properly calibrated and validated in two full scale systems operated for three years in real conditions.

The development of this model implies a considerable progress on the insight in nitrogen removal in FWSCWs and conclusions obtained in this study provide useful knowledge for maximizing nitrogen removal efficiency in FWSCWs.

The model includes the mechanisms related to heterotrophic and autotrophic microorganisms, phytoplankton and macrophytes. Immobility feature of the microorganisms was needed to be considered for properly reproducing observed concentrations in the effluent, so microorganisms were supposed to be attached in available surfaces. Aerobic and anoxic conditions were reproduced through diurnal and nocturnal oxygen oscillations, which are typical in hypertrophic water bodies. The effect of macrophyte uptake on nitrogen removal was simulated by means of the vegetation cover.

Additionally, the quantification of the influence of each mechanism in ammonium removal showed that the main process for ammonium removal was the growth of autotrophic microorganisms, whereas anoxic growth of heterotrophic microorganisms was the most important process for nitrate removal. Plant uptake removed a substantial amount of dissolved inorganic nitrogen, especially in the system where vegetation cover was higher. Even so, an important quantity of ammonium was recycled in this system by plant degradation so appropriate harvesting could increase ammonium removal.

Finally, future research would be necessary in order to improve organic matter modelling. Furthermore, more knowledge is needed for clarifying microorganisms distribution along the available surface in the system, which would allow to answer questions such as where processes take place into FWSCWs and how harvesting or losing macrophyte biomass affect to microorganisms community.

Acknowledgements

We would like to acknowledge the support of Confederación Hidrográfica del Júcar (CHJ, MMARM) and the staff members in *Tancat de la Pipa*. We also acknowledge the anonymous reviewers and the editor for their valuable comments to improve this paper.

References

Álvarez, J.A., Bécares, E., 2006. Seasonal decomposition of Typha latifolia in a free-water surface constructed wetland. Ecol. Eng. 28, 99–105. doi:10.1016/j.ecoleng.2006.05.001

Ambrose, R.B., Wool, T.A., Connolly, J.P., Schanz, R.W., 1988. WASP4, A Hydrodynamic and Water Quality Model - Model Theory, User's Manual, and Programmer's Guide.

APHA, 1991. Standard Methods for the Examination of Water and Wastewater. Stand. Methods 541.

Arheimer, B., Pers, B.C., 2016. Lessons learned? Effects of nutrient reductions from constructing wetlands in 1996–2006 across Sweden. Ecol. Eng. 1–11. doi:10.1016/j.ecoleng.2016.01.088

Asaeda, T., Karunaratne, S., 2000. Dynamic modeling of the growth of Phragmites australis: model description. Aquat. Bot. 67, 301–318. doi:10.1016/S0304-3770(00)00095-4

Galanopoulos, C., Lyberatos, G., 2016. Dynamic Modelling and design of free water surface constructed wetland systems 18.

Garcia, J., Rousseau, D.P.L., Morató, J., Lesage, E., Matamoros, V., Bayona, J.M., 2010. Contaminant removal processes in subsurface-flow constructed wetlands: a review. Crit. Rev. Environ. Sci. Technol. 40, 561–661. doi:10.1080/20016491089253

Gargallo, S., Martín, M., Oliver, N., Hernández-Crespo, C., 2016. Sedimentation and resuspension modelling in free water surface constructed wetlands. Ecol. Eng. doi:10.1016/j.ecoleng.2016.09.014

He, S.-B., Yan, L., Kong, H.-N., Liu, Z.-M., Wu, D.-Y., Hu, Z.-B., 2007. Treatment Efficiencies of Constructed Wetlands for Eutrophic Landscape River Water. Pedosphere 17, 522–528. doi:10.1016/S1002-0160(07)60062-9

Henze, M., Gujer, W., Mino, T., Loosdrecht, M. van, 2000. Activated Sludge Models ASM1, ASM2, ASM2d and ASM3. IWA Publishing.

Hernández-Crespo, C., 2013. Mid-term variation of vertical distribution of acid volatile sulphide and simultaneously extracted metals in sediment cores from Lake Albufera (Valencia, Spain). Arch. Environ. Contam. Toxicol. 65, 654–664. doi:10.1007/s00244-013-9941-1

Hernández-Crespo, C., Oliver, N., Bixquert, J., Gargallo, S., Martín, M., 2016. Comparison of three plants in a surface flow constructed wetland treating eutrophic water in a Mediterranean climate. Hydrobiologia 774, 183–192. doi:10.1007/s10750-015-2493-9

Hopkins, T., 1983. Quantitative analysis and simulation of Mediterranean coastal ecosystems: The Gulf of Naples, a case study. United Nations Educational, Scientific and Cultural Organization.

Kadlec, R.H., Knight, L., 1996. Treatment Wetlands, booksgooglecom. CRC Press, Boca Raton FL. doi:10.1201/9781420012514

Kadlec, R.H., Wallace, S.D., 2009. Treatment Wetlands, Second Edition.

Langergraber, G., 2008. Modeling of Processes in Subsurface Flow Constructed Wetlands: A Review. Vadose Zo. J. 7, 830. doi:10.2136/vzj2007.0054

Langergraber, G., Rousseau, D.P.L., García, J., Mena, J., 2009. CWM1: A general model to describe biokinetic processes in subsurface flow constructed wetlands. Water Sci. Technol. 59, 1687–1697. doi:10.2166/wst.2009.131

Langergraber, G., Šimůnek, J., 2005. Modeling Variably Saturated Water Flow and Multicomponent Reactive Transport in Constructed Wetlands. Vadose Zo. J. 4, 924. doi:10.2136/vzj2004.0166

Li, L., Li, Y., Biswas, D.K., Nian, Y., Jiang, G., 2008. Potential of constructed wetlands in treating the eutrophic water: Evidence from Taihu Lake of China. Bioresour. Technol. 99, 1656–1663. doi:10.1016/j.biortech.2007.04.001

Llorens, E., Saaltink, M.W., García, J., 2011. CWM1 implementation in

581 RetrasoCodeBright: First results using horizontal subsurface flow constructed
582 wetland data. Chem. Eng. J. 166, 224–232. doi:10.1016/j.cej.2010.10.065

583 Martín, M., Oliver, N., Hernández-Crespo, C., Gargallo, S., Regidor, M.C., 2013. The
584 use of free water surface constructed wetland to treat the eutrophicated waters
585 of lake L'Albufera de Valencia (Spain). Ecol. Eng. 50, 52–61.

586 Mburu, N., Sanchez-Ramos, D., Rousseau, D.P.L., van Bruggen, J.J.A., Thumbi, G.,
587 Stein, O.R., Hook, P.B., Lens, P.N.L., 2012. Simulation of carbon, nitrogen and
588 sulphur conversion in batch-operated experimental wetland mesocosms. Ecol.
589 Eng. 42, 304–315. doi:10.1016/j.ecoleng.2012.02.003

590 Mcbride, G.B., Tanner, C.C., 2000. Modelling biofilm nitrogen transformations in
591 constructed wetland mesocosms with fluctuating water levels. Ecol. Eng. 14, 93–
592 106. doi:10.1016/S0925-8574(99)00022-1

593 Oliver, N., Martín, M., Gargallo, S., Hernández-Crespo, C., 2016. Influence of
594 operational parameters on nutrient removal from eutrophic water in a
595 constructed wetland. Hydrobiologia 1–16. doi:10.1007/s10750-016-3048-4

596 Pálfy, T.G., Langergraber, G., 2014. The verification of the constructed wetland
597 model no. 1 implementation in HYDRUS using column experiment data. Ecol.
598 Eng. 68, 105–115. doi:10.1016/j.ecoleng.2014.03.016

599 Reddy, K.R., DeLaune, R.D., 2008. Biogeochemistry of wetlands: science and
600 applications. CRC press.

601 Reichert, P., 1998. AQUASIM 2.0 - User Manual. Computer Program for the
602 Identication and Simulation of Aquatic Systems. Swiss Federal Institute for
603 Environmental Science and Technology (EAWAG), Dubendorf.

604 Reichert, P., 1994. AQUASIM - A tool for simulation and data analysis of aquatic
605 systems. Water Sci. Technol. 30, 21–30.

606 Reichert, P., Boarchardt, D., Henze, M., Rauch, W., Shanahan, P., Somlyódy, L.,
607 Vanrolleghem, P., 2001. River Water Quality Model No.1. IWA Publishing.

608 Romero, J.A.J.A., Brix, H., Comín, F.A., 1999. Interactive effects of N and P on
609 growth, nutrient allocation and NH 4 uptake kinetics by Phragmites australis.
610 Aquat. Bot. 64, 369–380.

611 Rousseau, D.P.L., 2005. Performance of Constructed Treatment Wetlands : Model-
612 Based Evaluation and Impact of Operation and Maintenance Werking Van
613 Aangelegde Zuiveringsmoerassen : Modelgebaseerde Evaluatie En Impact Van.
614 Environ. Technol. Ghent University, Ghent, Belgium,.

615 Saeed, T., Sun, G., 2012. A review on nitrogen and organics removal mechanisms in
616 subsurface flow constructed wetlands: Dependency on environmental
617 parameters, operating conditions and supporting media. J. Environ. Manage.
618 112, 429–448.

619 Samsó, R., Garcia, J., 2013. BIO_PORE, a mathematical model to simulate biofilm
620 growth and water quality improvement in porous media: Application and
621 calibration for constructed wetlands. Ecol. Eng. 54, 116–127.

622 doi:10.1016/j.ecoleng.2013.01.021

623 Sánchez-Carrillo, S., Angeler, D.G., Álvarez-Cobelas, M., 2011. Freshwater wetland
624 eutrophication, in: Eutrophication: Causes, Consequences and Control. p. 394.

625 Tang, X., Huang, S., Scholz, M., Li, J., 2009. Nutrient Removal in pilot-scale
626 constructed wetlands treating eutrophic river water: Assessment of plants,
627 intermittent artificial aeration and polyhedron hollow polypropylene balls. Water.
628 Air. Soil Pollut. 197, 61–73. doi:10.1007/s11270-008-9791-z

629 Thomann, R. V, Fitzpatrick, J.J., 1982. Calibration and Verification of a Mathematical
630 Model of the Eutrophication of the Potomac Estuary. DC Department of
631 Environmental Sciences.

632 Wynn, T.M., Liehr, S.K., 2001. Development of a constructed subsurface-flow
633 wetland simulation model. Ecol. Eng. 16, 519–536. doi:10.1016/S0925-
634 8574(00)00115-4

635